94-GHz Pulsed Silicon IMPATT Oscillator Modeling

Stéphane Beaussart, Olivier Perrin, Marie-Renée Friscourt, and Christophe Dalle

***Abstract*— A new type of 94-GHz pulsed silicon impact avalanche and transit time (IMPATT) oscillator numerical modeling is described. It consists of a set of three models of increasing complexity; namely, a pure sine model, time-domain isothermal model, and time-domain electro-thermal model, which basically rely on a diode one-dimensional bipolar drift–diffusion model embedded in a time-domain circuit modeling. In this paper, they are first used to investigate the 94-GHz diode intrinsic operation and performance. Secondly, the load-impedance level has been optimized. In each case, the thermal behavior is especially considered. Thirdly, pulse-operation-simulation results are compared with experiments performed at Thomson CSF, Radars et Contre-Mesures, Elancourt, France. Finally, some improvements of the present modeling are discussed in Section VI.**

***Index Terms*—Macroscopic modeling, millimeter waves, pulsed IMPATT oscillator.**

I. Introduction

DESPITE the improvements of transistor performance, the silicon impact avalanche and transit time (IMPATT) diode still remains the most powerful semiconductor device for the realization of 94-GHz pulsed solid-state front-end transmitters capable of providing instantaneous RF power levels in the range of several tens of watts [1]. The RF operation of such oscillators shows specific features depending on the following diode intrinsic RF properties, bias conditions, and passive load–circuit frequency behavior.

1) The oscillator operates during periodic short pulses (duration less than 100 ns) with a low duty factor (several percent). Thus, the diode alternatively heats and cools. Due to the thermal inertia of its heat-sink, the diode operates under transient thermal conditions.
2) The IMPATT diode intrinsic RF operation is strongly nonlinear and temperature dependent. Indeed, on one hand, the electron and hole ionization rates determining the carrier generation rate by impact ionization are exponential functions of the electric-field intensity [2]. They decrease with the temperature. On the other hand, the carrier saturated velocities determine the electron and hole transit time and, consequently, the operating frequency. They are also decreasing functions of the operating temperature [3].
3) The IMPATT diode is biased under high current density (higher than 100 kA/cm^2). This yields important space-charge effects in the diode active zone, which influence its RF operation and performance.
4) The IMPATT diode large-signal operation emphasizes the nonlinear effects.
5) During one current pulse, the diode impedance level can present large instantaneous variations, while the passive load–circuit frequency behavior remains obviously fixed. This yields device–circuit interaction resulting in various effects such as instantaneous operating frequency chirp and variations of the emitted power level.

Despite the numerous theoretical works devoted to the IMPATT oscillators since its invention by Read in 1958, there is still lack of knowledge on the complex thermal and electrical transient operation of millimeter-wave high-power pulsed IMPATT oscillators [4]–[8]. This does not facilitate the designer's job, especially in the case of applications requiring high stability of both the operating frequency and RF output power level. Thus, the circuit tuning operation of such oscillators is complicated, to the detriment of the industrial production costs.

The purpose of this paper is to report on the modeling rather than the circuit design and optimization. The choice of a numerical model often results from a tradeoff between the computational effort and realism of the simulation. We have developed a set of three time-domain IMPATT oscillator models of increasing complexity. The most accurate of them is an electro-thermal one. These circuit models are based on a one-dimensional bipolar drift–diffusion numerical analysis of IMPATT diode. All these models are described in Section II. In Section III, the diode intrinsic 94-GHz monochromatic operation is investigated by means of the pure sine model. The influences of the RF voltage amplitude, dc-bias current density, and temperature are considered. In Section IV, the influences of both the load–circuit impedance and operating temperature are analyzed by means of continuous wave (CW) isothermal time-domain simulations. In Section V, theoretical results obtained by means of the time-domain electro-thermal oscillator model are compared with experiments performed at Thomson CSF, Radars et Contre-Mesures, Elancourt, France.

The observed good agreement confirms the potential advantage of such a simulation. Therefore, in Section VI, some improvements of the present modeling are proposed to yield a more accurate and exhaustive study.

Manuscript received December 30, 1996; revised October 21, 1997. This work was supported by the Direction des Recherches, Etudes et Techniques under Contract 94/160.

S. Beaussart, M.-R. Friscourt, and C. Dalle are with the IEMN–DHS, UMR CNRS 9929, 59652 Villeneuve d'Ascq Cedex, France.

O. Perrin is with Thomson CSF, Radars et Contre-Mesures, 78852 Elancourt Cedex, France.

Publisher Item Identifier S 0018-9480(98)07250-0.

II. Oscillator Modeling

A. IMPATT Diode Modeling

The IMPATT diode model is a numerical one-dimensional bipolar drift–diffusion model [9]. The use of such a theoretical model instead of an energy hydrodynamic one at frequencies as high as 94 GHz has been previously justified [9]. The solution of the partial differential equation system (see Appendix A) is performed by means of the finite-difference method. The whole semiconductor structure is considered, including the heavily doped ohmic contacts. This allows modeling of structures with realistic doping profiles. Boundary conditions are accurately obtained from near thermodynamic equilibrium conditions. Moreover, the residual current initializing the avalanche process at the beginning of each RF cycle is not influenced by the boundary conditions, but rather results from the diode RF operation.

B. Circuit Modeling

The time-domain electric circuit analysis is based on the solution of the integro-differential Kirchoff's voltage and current laws. It can be applied to any lumped linear or nonlinear circuit. This method requires the knowledge of the instantaneous volt–ampere characteristic that defines the specific electrical properties of each network branch. We have developed a time-domain IMPATT oscillator model in which the diode model is the previously described drift–diffusion one. The other circuit elements fundamentally consist of resistances, capacitances, inductances, and generators. All these elements are numerically modeled by means of explicit finite-difference schemes (see Appendix B). This assumption is justified by the low time-increment value imposed by the semiconductor model numerical stability criteria [10]. Indeed, the time increment is limited to about 10^{-14} s in the case of our IMPATT diode model. Thus, in our time-domain circuit-modeling, a circuit is divided into two parts: the semiconductor devices considered as nonlinear elements and the rest of the circuit, the behavior of which is considered as linear. This allows us to reduce the number of circuit equation variables to those driving the nonlinear semiconductor elements (namely, in our modeling, the diode applied voltage) to the benefit of the computational efficiency. Thus, when the Kirchoff's equation numerical form is expressed, the solution is performed at each time increment by means of the iterative Newton–Raphson method.

Our IMPATT oscillator embedding circuit simply consists of an ideal current generator supplying the diode, which is connected to the passive RF load–circuit. Three different models of increasing complexity have been derived from this general model.

1) Isothermal CW Pure Sine or "Frequency-Domain" Model: The simplest oscillator model relies on the assumption that the passive RF load–circuit presents an ideal infinite quality (Q)-factor. The oscillator model is then simplified to the use of the semiconductor device model in which the diode applied voltage is pure sine and the total current is determined by the carrier dynamics. The simulation is performed until stable waveforms are reached accounting for the dc-current bias conditions. Fourier analysis of the current and voltage time-domain waveforms can then determine the emitted RF power, associated conversion efficiency, and diode impedance level in the frequency domain. Obviously, the results are realistic only if the oscillation condition can be actually obtained in practice: the load impedance must be feasible with passive circuit technology. This model is well suited for systematic investigations of the physical phenomena determining the device operation, definition of the intrinsic RF performance, and diode structure optimization [11].

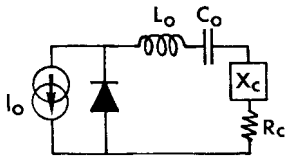

Fig. 1. IMPATT oscillator equivalent scheme.

2) Isothermal Time-Domain Oscillator Model: The pure sine oscillator model relies on the assumption that the passive load circuit presents an infinite Q-factor. However, when a more realistic finite Q-factor is considered, this assumption can no longer be made upon the circuit signal waveform and operating frequency. Consequently, the Kirchoff's equations have to be solved. Fig. 1 illustrates the oscillator circuit we consider. The bias circuit is an ideal current generator. A simple RF load–circuit configuration is considered in this preliminary study. It consists of an R–L–C lumped-element circuit. The L_0–C_0 94-GHz resonant circuit is used to isolate the dc from the RF circuit and to modify the external Q-factor. The load impedance consists of the R_c resistance and the X_c reactive passive element, which match the diode impedance at the expected operating frequency.

Although the R–L–C circuit does not perfectly account for the complex frequency behavior of a real load circuit, it is realistic in a limited frequency band around 94 GHz. Whatever the frequency may be, the load resistance level is constant and its value is low. This feature certainly favors the parametric operation. Indeed, the R–L–C circuit offers to the diode a wider and more continuous range of potential stable operating points than a real load circuit presenting a more limited number of stable operating points. Thus, the R–L–C load circuit constitutes a simple means to investigate some features of the diode parametric operation. Finally, a last advantage of the R–L–C load circuit is that the oscillator modeling remains fast enough to allow systematic investigations.

Time-domain modeling has been used to optimize the 94-GHz load-impedance level and to define the corresponding bias conditions for a high-power free-running operation over the 300–600-K temperature range. In comparison, the pure sine model only allows investigation of 94-GHz intrinsic diode operation under restricted dc bias and matching conditions. Moreover, time-domain modeling naturally accounts for nonlinear effects resulting from the active-device–external-circuit interaction, such as the back bias effect or parametric operation.

The simulations are performed for a fixed operating temperature from the transient until CW operation is reached. Note

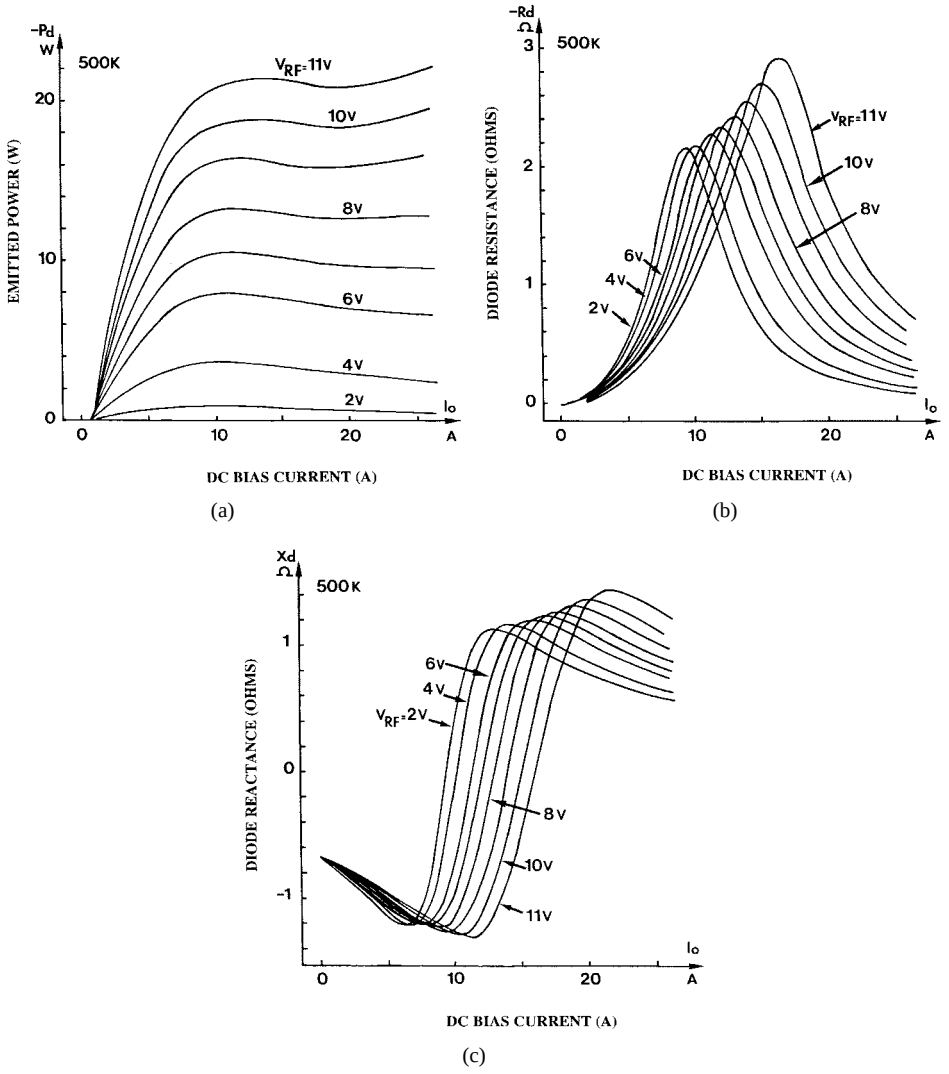

Fig. 2. (a) 94-GHz emitted power, (b) impedance level, and (c) as a function of the dc-bias current at 500 K for different diode-junction temperatures.

that our modeling does not account for noise. The oscillation starts up because of the pertubation induced by the bias-current-pulse rise up. The signals are then Fourier analyzed. Due to the finite load circuit Q-factor, the fundamental operating frequency is not *a priori* imposed. Consequently, both the X_c reactive passive element and dc-bias current values must be adjusted for 94-GHz operation.

3) Time-Domain Electro-Thermal Oscillator Model: In order to improve the realism of the pulsed IMPATT oscillator modeling, a new time-domain electro-thermal model has been developed. This model relies on the previously described time-domain oscillator model, which is coupled to the numerical solution of the one-dimensional heat-diffusion equation. This equation is solved by means of a finite-difference-method-based algorithm [12]. The simulation is performed from the diode gold/N^+ top layer up to the copper heat-sink (see Appendix C). Thermostatic boundary conditions have been considered. The ambient temperature value is imposed at the thermal model boundaries. The carrier transport parameters are consistently adjusted during the simulation according to the instantaneous heat power dissipation. Thus, the electro-thermal oscillator model finally accounts for the main feature of the pulsed IMPATT oscillator operation, namely:

1) frequency behavior of the passive load–circuit is taken into account;
2) IMPATT diode highly nonlinear behavior, large-signal, and transient operation is accurately described;
3) diode operating temperature dependence is selfconsistently taken into account according to the instantaneous heat power dissipation.

This model is well suited for the optimization of the bias current pulse waveform and for the comparison with experimental measurements.

III. Diode 94-GHz Intrinsic Operation

Systematic investigations have been performed in order to determine the diode 94-GHz intrinsic RF performance and impedance level in pure sine operating mode, as a function of the main operating parameters, namely:

1) dc-bias current density;
2) operating junction temperature;
3) the RF voltage amplitude.

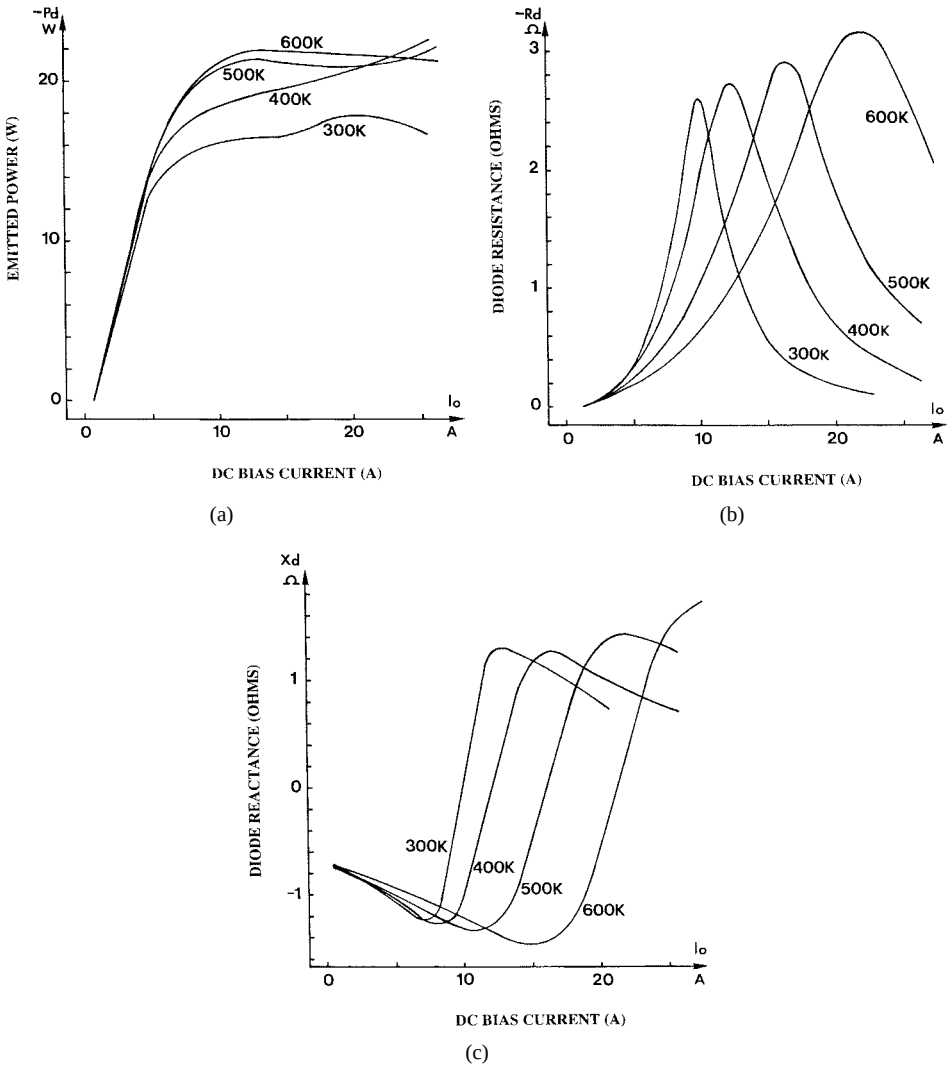

Fig. 3. (a) 94-GHz emitted power, (b) impedance level, and (c) as a function of the dc-bias current under large-signal operation for different diode-junction temperatures.

The dc-bias current density has been varied from 10 to 250 kA/cm^2. The influence of the operating-junction temperature has been studied over the 300–600-K range because the temperature can widely vary during a pulse (more than 100 K). Moreover, the oscillator must be capable of operating over a large ambient temperature range. The RF voltage modulation has been varied between 10%–60%. To a certain extent, this parameter accounts for the influence of the load-impedance level. The p^+- p-n-n^+ epitaxial structure parameters of a flat doping-profile double-drift 94-GHz silicon IMPATT diode, the p and n active zone lengths L_n and L_p, and the corresponding N_d and N_a doping levels, have been previously optimized [13]. Thus, this study illustrates typical results for a near optimum structure ($N_a = N_d = 2 \times 10^{23}$ m^{-3}, $L_N = L_P = 0.15$ μm). The results are presented for a standard diode area of 10^{-8} m^2. Fig. 2 represents the diode emitted power and impedance level variations as a function of the dc-bias current for various RF voltage amplitudes at an operating temperature of 500 K. These results show that the emitted power level increases from the initial current up to about 10 A, and then tends to saturate at its maximum value. Emitted power levels higher than 20 W can be achieved for the highest RF voltage amplitudes. The negative resistance level peaks for a dc-bias current corresponding to the transition of the reactance between the capacitive and inductive states. Both the maximum negative resistance level and corresponding dc-bias current increase with the RF voltage amplitude. The diode impedance evolutions point out a resonance-like effect, depending on the dc-bias current value. This resonance effect occurs when the inductive behavior of the carrier generation process by the avalanche effect and capacitive behavior of the diode internal field zone mutually compensate (avalanche resonance).

Fig. 3 shows the evolutions of the diode emitted power and the impedance level as a function of the dc-bias current for a nearly constant optimum RF voltage modulation rate and various operating junction temperature values. The maximum achievable power level substantially varies with the temperature. Indeed, because of the decrease of the electron and hole saturation velocities with the temperature, and according to the low p and n transit zone lengths, the diode is optimized to operate at high operating temperature, namely in the 500–600-K range, rather than at temperatures in the 300–400-K range.

From a general point of view, the results show that when all the operating parameters are taken into account, the diode

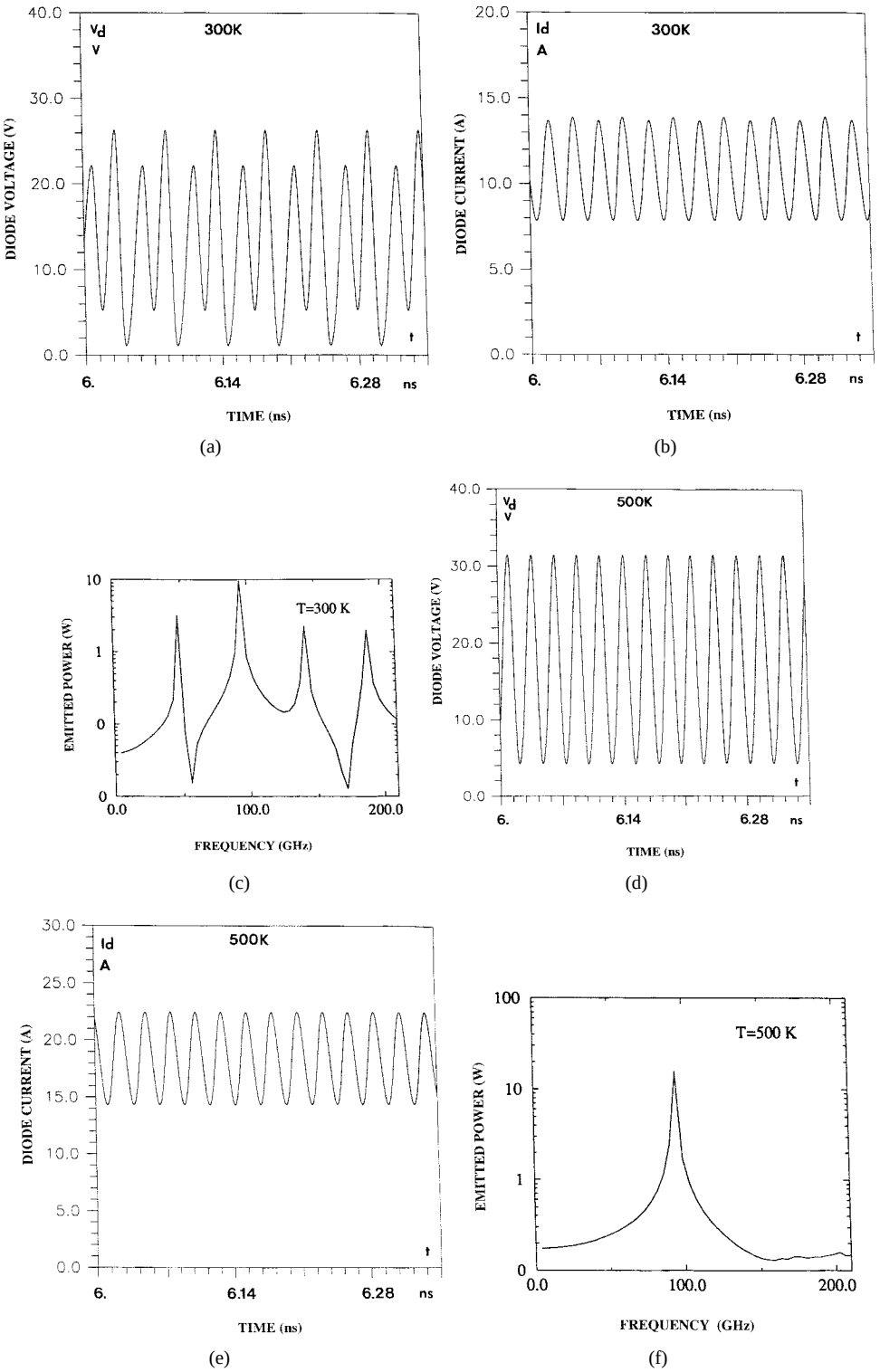

Fig. 4. (a) and (d) Diode voltage and current. (b) and (e) Time-domain waveforms. (c) and (f) Oscillator output power frequency spectrum. (a)–(c) Under CW steady-state operation at 300 and (d)–(f) 500 K.

impedance level can vary in a large range. For a designer, this complicates the choice of the optimum 94-GHz load-impedance level. This is especially the case for applications requiring a good stability of both the instantaneous emitted power level and operating frequency. Optimum matching conditions correspond to bias current values close or slightly below the resonance current value (for which the diode still behaves as a capacitance). These matching conditions indeed yield the highest dc-to-RF conversion-efficiency values.

IV. Load-Impedance-Level Optimization

CW isothermal time-domain simulations have been performed to determine the optimum 94-GHz load-impedance

level leading to high-power generation over the 300–600-K temperature range. First, approximations have been deduced from the previous pure-sine operating-mode simulations. The bias dc current has been adjusted to impose a fundamental operating frequency close to 94 GHz. The passive load–circuit external Q-factor has been adjusted (especially the reactance versus frequency evolution $\partial X/\partial\omega$) following values obtained by means of computer-aided design (CAD) simulations of both the practically used waveguide cavity and diode package elements [14]. The simulations have pointed out parametric effects leading to power generation at several frequencies. In most of the cases, it appears that all the signals were harmonic from the lowest frequency-induced signal (however, it must be noticed that the lowest frequency-induced signal is not always a 47-GHz subharmonic signal). This behavior occurs for this diode, especially at low operating temperatures, namely in the 300–400-K range. Fig. 4 is a comparison of the diode CW steady-state operation at 300 and 500 K. It shows the typical evolutions of the time-domain voltage V_d across the diode terminals and the corresponding current waveform I_d. At 300 K, the diode voltage waveform appears strongly distorted by the induced parametric signals, while the current one is approximately sinusoidal. Thus, the power generated at these frequencies remains low as compared to the fundamental one, as clearly illustrated by the power frequency spectrum. At 500 K, the diode operation is quite monochromatic. A plausible explanation comes from the fact that the diode structure considered in the simulation is optimized to operate at 94 GHz for a 500-K temperature [13]. At a lower operating temperature such as 300 K, the carrier transit time is lower, and the diode is easily capable of oscillating at frequencies higher than 94 GHz if the matching conditions allow it. The spurious signal is then mixed with the fundamental frequency, leading to down conversion. This temperature-induced parametric effect has been systematically observed in our simulations. However, this feature constitutes only one of the aspects of the complex IMPATT oscillator parametric operation, which can result from dc-induced instabilities [8], broad-band diode–load circuit interaction [15], thermal-induced instabilities, etc. The purpose of this paper is not to exhaustively investigate these effects.

Fig. 5 shows the 94-GHz CW RF performance and corresponding dc-bias current as a function of the operating temperature for different 94-GHz load-impedance levels. The results point out a near-optimum load-impedance level corresponding to a 3-Ω resistance value and a 1-Ω reactance. This impedance level is consistent with those previously calculated from the pure sine model. Moreover, the results show that the oscillator can also operate with load-impedance level higher than those predicted by the pure sine model. This feature could influence the choice of the optimum diode area for high-power generation.

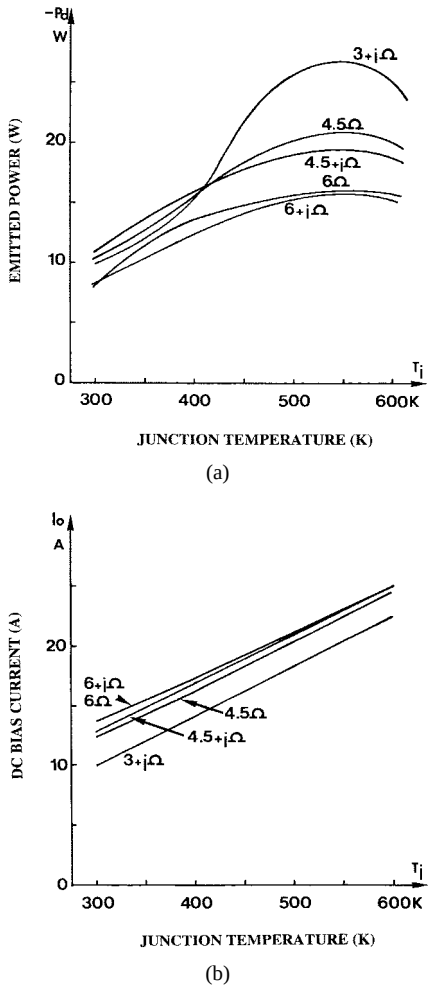

Fig. 5. (a) 94-GHz CW RF emitted power. (b) Corresponding dc-bias current as a function of the diode temperature for different load-impedance levels.

V. Pulse-Operation Simulation

Since the description of the cooling periods between the pulses presents no interest in our study, only mono-pulse-operation simulations have been performed by means of the electro-thermal model. The results have been compared to experimental ones performed under steady-state periodic pulse operation at Thomson CSF, Radars et Contre-Mesures. The parameters of the diode realized at Thomson, namely its doping profile and area, have been introduced in the model. In the same way, the heat-sink theoretical parameters have been defined according to the real diode and circuit structure. Due to the lack of information on the experimental 94-GHz diode load-impedance level (and associated Q-value), this parameter has been theoretically determined, as previously described by means of CW isothermal time-domain simulations. A near optimum value of $Z_c = (2.65 + j0.88)\ \Omega$ at 94 GHz has been found. The simulations are performed on a duration of 100 ns. The oscillator is considered as initially relaxed at the ambient temperature equal to 300 K. The bias current pulse waveform has been approximated according to the experimental measurements [see Fig. 6(a)]. Fig. 6(b) shows the temporal evolution of the 94-GHz detected output power. These experimental results can be compared to the theoretical ones. Fig. 6(c) and (d), respectively, show the theoretical temporal evolutions of the "instantaneous" fundamental operating frequency and the diode-junction temperature. From a general point of view, the comparison shows that the predicted duration of operation around 94 GHz is consistent with the experimental one. However, we observe some differences

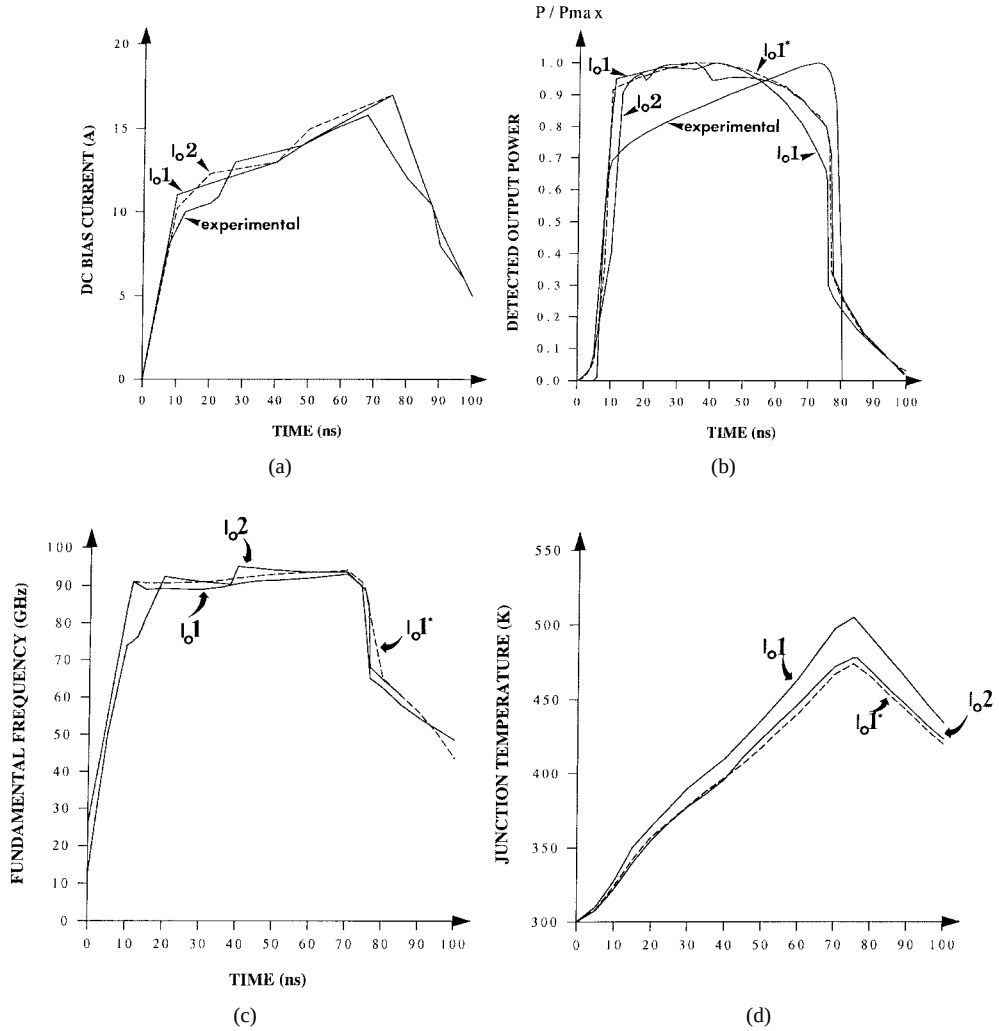

Fig. 6. (a) Comparison of the experimental and theoretical evolutions of the bias current waveform. (b) The 94-GHz time-domain detected output power. Theoretical temporal evolutions of the (c) "instantaneous" fundamental frequency and (d) diode-junction temperature.

concerning the output-power pulse waveforms. They can be attributed to several parameters. Firstly, the simulations have been performed up to now under free-running operation, while the experimental results have been measured under injection-locked operation. This operation should be included to account for the coupling between the oscillator and injected RF source. This complex problem is not covered in this paper. Secondly, the simulations have shown the sensitivity of the results according to the bias current pulse waveform approximation. Indeed, the instantaneous oscillator operation results from both the diode instantaneous-bias current and junction temperature values according to the matching conditions imposed by the load–circuit frequency behavior. Thirdly, some differences between the measured diode-doping profile and the theoretical one can always be a source of discrepancy. Finally, we have systematically observed, at the end of the pulse, a more rapid and pronounced decrease of the theoretical 94-GHz-power waveform, as compared to the experimental one. A plausible explanation may be that the junction temperature rise is slightly overestimated because of the simple one-dimensional thermal model. This assumption has been confirmed by means of comparison obtained from a full three-dimensional (3-D) thermal model [16]. In order to give an idea of the influence of the dissipated power, we have represented in Fig. 6 (curves marked by $I_0 1^*$) the theoretical results obtained when only 90% of the dissipated power is taken into account for the calculation of the junction temperature. Finally, we must note that the initial theoretical temperature is 300 K, while it is certainly higher in practice (350 K).

VI. Conclusion

The first theoretical results of a preliminary study devoted to the optimization of 94-GHz high-power pulsed silicon IMPATT oscillators have been presented. A new time-domain electro-thermal oscillator model has been described. The diode intrinsic 94-GHz operation has been investigated under sinusoidal drive. The load-impedance level was next optimized. In each case, the thermal point of view has been especially investigated. Finally, pulse-operation simulations have been compared to experimental measurements. A good agreement has been demonstrated. Thus, our numerical modeling asserts itself as an accurate and efficient tool in the theoretical study

of millimeter-wave pulsed oscillators. However, despite its potential, the model can be still significantly improved. Due to the one-dimensional thermal model, the diode-junction temperature rise is overestimated. Thus, a thermal model including a 45° heat-diffusion cone through the heat-sink is currently under development. However, because of the device resolution symmetry, a full 3-D cylindrical coordinate heat-diffusion model could be the most accurate and efficient solution. Moreover, up to now, a simple R–L–C RF load–circuit has been considered. This assumption constitutes one of the main limitation of this model. Indeed, the frequency behavior of this circuit is far from that of the reduced-height waveguide cavity. Moreover, the influence of the diode connection and package elements must be taken into account. Thus, a more realistic model of the passive load–circuit is currently under development. It basically relies on a 3-D electromagnetic modeling by means of the HFSS CAD model. This model can be used to determine the frequency evolution of the load–circuit impedance from which its impulse response can be deduced. This final result is then directly usable in the time-domain oscillator model [17]. Thus, the realism of our modeling should be improved. However, one must bear in mind that these potential improvements should be carried out at the expense of computational efficiency. Indeed, the goal of this study is not only to design and optimize a high-power and stable pulse IMPATT oscillator, but especially to try to simplify the practical use and tuning procedure for efficient and lower cost industrial production.

APPENDIX A
DEVICE MODELING

The classical set of equations solved in our drift–diffusion modeling contains the current, continuity, and Poisson's equations. Its normalized form is as follows [9]:

Continuity equations:

$$\frac{\partial n}{\partial t} = \frac{\partial J_n}{\partial x} + g - u$$
$$\frac{\partial p}{\partial t} = -\frac{\partial J_p}{\partial x} + g - u.$$

Current densities:

$$J_n = \mu_n\left(nE + \frac{\partial n}{\partial x}\right)$$
$$J_p = \mu_p\left(pE - \frac{\partial p}{\partial x}\right).$$

Poisson's equation:

$$\frac{\partial^2 V}{\partial x^2} = N_d - N_a + p - n$$
$$E = -\frac{\partial V}{\partial x}.$$

Generation rate by impact ionization:

$$g = \alpha_n|J_n| + \alpha_p|J_p|.$$

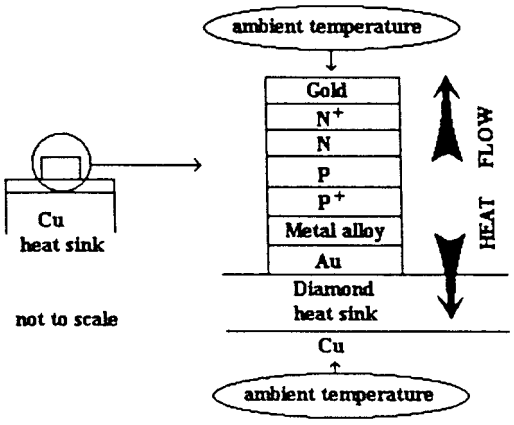

Fig. 7. Oscillator thermal modeling.

Recombination rate:

$$u = \frac{np - 1}{\tau_n(p+1) + \tau_p(n+1)}.$$

Total current:

$$J(t) = J_n + J_p + \frac{\partial E}{\partial t}$$

x is the space coordinate, t the time. N_d and N_a are the net donor and acceptor densities. n is the electron density and p the hole density, n and p indices denote quantities of electrons and holes, respectively. μ is the carrier mobility, E is the electric-field strength, V the electrostatic potential. J is the current density, g the impact-ionization rate, α the impact-ionization coefficient, and τ is the carrier lifetime.

APPENDIX B
LINEAR ELEMENTS MODELING

We use the following difference schemes for capacitive and inductive elements:

Voltage across a resistance R:

$$V_R^k = R \bullet I_R^{k-1}.$$

Voltage across an inductance L:

$$V_L^k = L \bullet \frac{I_L^k - I_L^{k-1}}{\Delta t}.$$

Voltage across a capacity C:

$$V_C^k = V_C^{k-1} + I_C^k \bullet \frac{\Delta t}{C}$$

where Δt is the time-increment value, and the k exponent denotes the time iteration such that $t = k \cdot \Delta t$.

The circuit-equation iterative sequence resolution is as follows:

$I_d^k = f(V_d^k)$, determined by the diode numerical model

$I_C^k = I_0 - I_d^k$

$V_C^k = V_C^{k-1} + I_C^k \bullet \dfrac{\Delta t}{C}$

$F^k = V_d^k - L \bullet \left(\dfrac{I_C^k - I_C^{k-1}}{\Delta t}\right) - V_C^k - R \bullet I_C^k$,

solved by Newton–Raphson method.

APPENDIX C
HEAT-DIFFUSION EQUATION

We solve the one-dimensional heat-diffusion equation

$$\frac{\partial}{\partial x}\left(\kappa S \frac{\partial T}{\partial x}\right) = \rho C S \frac{\partial T}{\partial t} - PS$$

where:

- T local temperature at the instant t;
- κ thermal conductivity;
- C specific heat;
- ρ density;
- P power dissipated per unit volume;
- S diode area;

in Fig. 7.

REFERENCES

[1] W. Behr and J. F. Luy, "High power operation mode of pulsed IMPATT diodes," *IEEE Electron Device Lett.*, vol. 11, pp. 206–208, May 1990.

[2] W. N. Grant, "Electron and hole ionization rates in epitaxial silicon at high electric fields," *Solid State Electron*, vol. 16, pp. 1189–1203, 1973.

[3] C. Jacoboni, C. Canali, G. Ottaviani, and A. Alberigi Quaranta, "A review of some charge transport properties of silicon," *Solid State Electron*, vol. 200, pp. 77–79, 1977.

[4] T. T. Fong and H. J. Kuno, "Millimeter-wave pulsed IMPATT sources," *IEEE Trans. Microwave Theory Tech.*, vol. MTT-27, pp. 492–500, May 1979.

[5] L. H. Holway, "Transient temperature behavior in pulsed double drift IMPATT diodes," *IEEE Trans. Electron Devices*, vol. ED-27, pp. 435–442, Feb. 1980.

[6] R. K. Mains, G. I. Haddad, B. Bowling, and M. Afendykiw, "Dynamic behavior of pulsed IMPATT oscillators," *IEEE Trans. Microwave Theory Tech*, vol. MTT-32, pp. 208–212, Feb. 1984.

[7] U. C. Ray and A. K. Gupta, "Intrapulse frequency variation in a W-band pulsed IMPATT diode," *Microwave J.*, pp. 238–244, 1994.

[8] L. Gaul and M. Claasen, "Pulsed high power operation of p^+pnn^+ avalanche diodes near avalanche resonance for mm-wave oscillators," *IEEE Trans. Electron Devices*, vol. 41, pp. 1310–1318, Aug. 1994.

[9] C. Dalle and P. A. Rolland, "Drift–diffusion model versus energy model for millimeter-wave IMPATT diodes modeling," *Int. J. Numer. Modeling*, vol. 2, pp. 61–73, 1989.

[10] C. Dalle, P. A. Rolland, and M. R. Friscourt, "Time-domain numerical modeling of microwave nonlinear circuits," *Int. J. Numer. Modeling*, vol. 5, pp. 41–52, 1992.

[11] C. Dalle, P. A. Rolland, and G. Lleti, "Flat doping profile double-drift silicon IMPATT for reliable CW high power high efficiency generation in the 94-GHz window," *IEEE Trans. Electron Devices*, vol. 37, pp. 227–236, Jan. 1990.

[12] F. T. Wenthen, "Computer-aided thermal analysis of power semiconductor devices," *IEEE Trans. Electron Devices*, vol. ED-17, pp. 765–770, Sept. 1970.

[13] P. A. Rolland, C. Dalle, and M. R. Friscourt, "Physical understanding and optimum design of high-power millimeter-wave pulsed IMPATT diodes," *IEEE Electron Device Lett.*, vol. 12, pp. 221–223, May 1991.

[14] S. Beaussart, "Contribution à l'étude du fonctionnement et à l'optimization des oscillateurs ATT au silicium de forte puissance en régime d'impulsions courtes à 94 GHz," Ph.D. dissertation, Univ. Lille, Lille, France, Dec. 1997.

[15] Brackett, "The elimination of tuning induced burnout and bias circuit oscillations in IMPATT oscillators," *BSTJ*, vol. 52, pp. 272–306, 1973.

[16] Y. Perreal, "Etude thermique: Diode IMPATT 94 GHz," Thomson-LCR, private communication, 1995.

[17] W. J. Evans and D. L. Scharfetter, "Characterization of avalanche diode TRAPATT oscillators," *IEEE Trans. Electron Devices*, vol. ED-17, pp. 397–404, May 1970.

Stéphane Beaussart was born in Hazebrouck, France, in 1967. He received the M.S. degree in electrical engineering and the Ph.D. degree in electronics from the University of Lille, Lille, France, in 1993 and 1997, respectively.

While working toward the Ph.D. degree, he worked in association with Thomson Radar and Counter Measure, Elancourt, France, where he was involved in the study of operating mode and optimization of high-power 94-GHz pulsed silicon IMPATT oscillators. He then joined the Integrated Semiconductor Business Unit, M/ACOM (a division of AMP Inc.), Lowell, MA, where he is currently working on GaAs MESFET and pHEMT modeling used in MMIC design.

Olivier Perrin was born in France, in 1963. He received the engineering degree from the Institut National des Télécommunications, Evry, France, in 1986, and the Ph.D. degree in electronics from the University of Paris Sud, Paris, France, in 1991.

In 1991, he joined the Microwave Laboratory, Thomson-CSF Radar and Countermeasure, Elancourt, France. He is currently involved in the design of microwave and millimeter-wave equipments.

Marie-Renée Friscourt was born in Berck, France, in 1957. She received the doctorat ès sciences physiques degree from the University of Lille Flandres Artois, Lille, France, in May 1985

In 1979, she joined the Centre Hyperfréquences et Semiconducteurs, Lille, France. Since October 1982, she has been with the Centre National de la Recherche Scientifique (CNRS), Villeneuve d'Ascq, France, where she works in the field of millimeter-wave active devices.

Christophe Dalle received the doctorat d'Université and the Habilitation à diriger des Recherches degrees from the University of Lille, Lille, France, in 1986 and 1992, respectively.

In 1982, he joined the Centre Hyperfrequences et Semiconducteurs. Since 1986, he has been with the Centre National de la Recherche Scientifique (CNRS), Villeneuve d'Ascq, France, as a Chargé de Recherche. From September 1989 to August 1990, he was a Research Fellow of the Alexander von Humboldt Foundation at the Lehrstuhl für allgemeine Elektrotechnik und angewandte Elektronik, Technical University of Munich, Munich, Germany, where he was involved in the modeling of millimeter-wave TUNNETT diodes. His research activities are mainly concerned with the time-domain physical modeling of semiconductor devices and related circuits for millimeter-wave and optronic applications.